Shapes of Dendrimers from Rotational-Echo Double-Resonance NMR

Karen L. Wooley,* Christopher A. Klug,[†] Kenzabu Tasaki,[‡] and Jacob Schaefer

Contribution from the Department of Chemistry, Washington University, St. Louis, Missouri 63130

Received July 5, 1996[⊗]

Abstract: The solid-state shape, size, and intermolecular packing of a fifth-generation dendritic macromolecule were determined by a combination of site-specific stable-isotope-labeling, rotational-echo double-resonance (REDOR) NMR and distance-constrained molecular dynamics simulations. REDOR experiments measured dipolar couplings between ^{13}C atoms located near the chain ends and an ^{19}F label placed at the core of benzyl ether dendrimers (generations 1−5) based on 3,5-dihydroxybenzyl alcohol as the monomeric repeat unit. Intramolecular $^{13}C-^{19}F$ coupling was distinguished from intermolecular coupling by dilution with nonlabeled dendrimer. The average intramolecular $^{13}C-^{19}F$ distances for generations 3−5 were each approximately 12 Å, which indicates inward-folding of chain ends with increasing generation number. The average intermolecular $^{13}C-^{19}F$ dipolar coupling decreased with increasing generation number, consistent with decreased interpenetration for larger dendrimers. The measured intra- and intermolecular distances for the fifth-generation dendrimer were used as constraints on energy minimizations and molecular dynamics simulations, which resulted in visualizations of the dendrimer packing and an estimate of density in the solid state.

Introduction

Polymers whose main chains branch at each repeat unit have been given the name dendritic macromolecules[1−4] because the chain backbone has many ends and resembles the branches of a tree. This structural architecture of dendritic macromolecules imparts highly interesting material properties. Light-scattering measurements[5] have shown that dendritic poly(benzyl ether)s are more compact than linear random-coil polymers of equivalent molecular weight. In solution, dendrimers have unusually low intrinsic viscosities[6] that decrease with increasing molecular weight. These observations lead to the conclusions that dendritic macromolecules possess globular shapes and lack intermolecular entanglements. In addition, solvatochromic studies of poly-(benzyl ether) dendrimers,[7] involving the placement of a solvent-sensitive chromophoric probe at the focal point, have revealed that a unique microenvironment exists near the core. This result suggests that the center of the dendrimer is engulfed by the branching repeat units and chain ends.

The employment of this interior site for catalysis[8] or transport has been suggested in the design of protein-like structures. Several reports have appeared,[9−11] detailing the encapsulation of porphyrins by dendrimers to generate synthetic mimics of electron transfer proteins. The recent demonstration of efficient coupling between chain ends and the core for layered electroluminescent dendrimers is consistent with the encapsulation of the core.[12] Meijer's dendritic box[13] has illustrated the feasibility of temporary and selective encapsulation of small molecules within the core of dendrimers. Poly(amidoamine) dendrimers are being explored for various biological applications, including their ability to act as agents that complex and transport DNA into eukaryotic cells.[14] Applications for dendritic structures as catalysts, conducting polymers, lubricants, and coatings attempt to take advantage of the large number of chain ends or the lack of chain entanglements.[15,16]

The composition of a dendrimer is the same as that of a linear polymer with a repeating side chain that is equivalent to the functional group of the dendrimer chain end. Therefore, the extraordinary properties that dendrimers exhibit must result from structural constraints imposed by the branching and not from the number of chain end functional groups. The conformation, shape, and packing of dendrimers are issues that have been debated for several years. A number of theoretical approaches have been proposed to describe the dendritic structure, in particular, the location of the chain ends. A self-consistent mean-field analysis by de Gennes and Hervet[17] placed chain ends at the periphery of the dendrimer and found a density maximum on the surface. In contrast, the computer simulation

(1) Newkome, G. R., Ed.; *Advances in Dendritic Macromolecules;* JAI Press, Ltd.: Greenwich, CT, 1994, 1995; Vols. 1−2.

(2) Fréchet, J. M. J. *Science* **1995**, *267*, 112.

(3) Tomalia, D. A.; Naylor, A. M.; Goddard, W. A., III *Angew. Chem.* **1990**, *102*, 119; *Angew. Chem., Int. Ed. Engl.* **1990**, *29*, 138.

(4) Ardoin, N.; Astruc, D. *Bull. Soc. Chim. Fr.* **1995**, *132*, 875.

(5) Hawker, C. J.; Fréchet, J. M. J. *J. Am. Chem. Soc.* **1990**, *112*, 7638.

(6) Mourey, T. H.; Turner, S. R.; Rubinstein, M.; Fréchet, J. M. J.; Hawker, C. J.; Wooley, K. L. *Macromolecules* **1992**, *25*, 2401.

(7) Hawker, C. J.; Wooley, K. L.; Fréchet, J. M. J. *J. Am. Chem. Soc.* **1993**, *115*, 4375.

(8) Miedaner, A.; DuBois, D. L. *ACS PMSE Proc.* **1995**, *73*, 279.

(9) Jin, R.-H.; Aida, T.; Inoue, S. *J. Chem. Soc., Chem. Commun.* **1993**, 1260.

(10) Dandliker, P. J.; Diederich, F.; Gross, M.; Knobler, C. B.; Louati, A.; Sanford, E. M. *Angew. Chem.* **1994**, *106*, 1821; *Angew. Chem., Int. Ed. Engl.* **1994**, *33*, 1739.

(11) Pollak, K. W.; Leon, J. W.; Fréchet, J. M. J. *ACS PMSE Proc.* **1995**, *73*, 333.

(12) Wang, P.-W.; Liu, Y.-J.; Devadoss, C.; Bharathi, P.; Moore, J. S. *Adv. Mater.* **1996**, *8*, 237.

(13) Jansen, J. F. G. A.; Meijer, E. W.; de Brabander-van den Berg, E. M. M. *J. Am. Chem. Soc.* **1995**, *117*, 4417.

(14) Bielinska, A.; Kukowska-Latallo, J.; Piehler, L. T.; Tomalia, D. A.; Spindler, R.; Yin, R.; Baker, J. R., Jr. *ACS PMSE Proc.* **1995**, *73*, 273.

(15) O'Sullivan, D. A. *Chem. Eng. News* **1993**, *72* (Aug. 16), 20.

(16) Service, R. F. *Science* **1995**, *267*, 458.

(17) de Gennes, P. G.; Hervet, H. *Physique: LETTRES* **1983**, *44*, L-351.

of kinetic starburst growth by Lescanec and Muthukumar[18] allowed for inward-folding of the chain ends, which resulted in a density maximum between the assumed dense core and the periphery. Monte Carlo calculations performed by Mansfield and Klushin[19] found the chain ends to be distributed throughout the structure and revealed a density maximum midway between the center of mass and the periphery. Molecular dynamics simulations by Naylor *et al.*[20] predicted open structures and a decreasing aspect ratio (more spherical shape) with increasing generation number. Molecular dynamics simulations which allowed varying solvent quality recently reported by Murat and Grest[21] found significant inward-folding of chain end groups, a high-density region near the central core for all of the solvents, and increasing overall dendrimer density with decreasing solvent quality.

Solution-state characterizations of dendrimers[5−7] generally support the presence of a globular shape with the chain ends accessible to the surface. However, details of the precise shape and chain end locations remain uncertain. Melt−viscosity measurements of dendrimers[22] have shown that the increase in viscosity with increasing molecular weight is less for dendrimers than for the corresponding linear polymers. Much less solid-state characterization has been performed. Liquid crystalline dendrimers[23] reorient faster and at lower electric and magnetic fields than their linear counterparts. Atomic force microscopy[24] has shown that thin films of dendritic materials are easily machined at lower tip forces than are films of linear polymers. Although these results suggest a general lack of dendrimer entanglement, quantitative data describing the size, shape, and packing of dendrimers are still needed to understand fully their structure and to aid in the design of dendrimers for specific applications.

In this study, rotational-echo double-resonance (REDOR) solid-state nuclear magnetic resonance (NMR) spectroscopy[25] was used as a direct-measurement technique to characterize a series of stable-isotope-labeled poly(benzyl ether) dendrimers. REDOR provides a direct measure of heteronuclear dipolar coupling between isolated pairs of labeled nuclei. The dipolar interaction between two spins depends on the inverse cube of the internuclear distance, on the orientation of the internuclear vector with respect to the applied static magnetic field, and on the magnetic moments of the two nuclei. That is, the dipolar coupling depends both on space and spin coordinates. Magic angle sample spinning suppresses the dipolar interaction by averaging over the space coordinates. This averaging process can be defeated and the dipolar coupling partially restored by a competing averaging using rotor-synchronized radio-frequency pulses, which operate exclusively on the spin coordinates. The space- and spin-averaging processes are both coherent and are of comparable frequency; therefore, their combination produces destructive interference of averaging leading to recoupling. The extent of the interference is a measure of the dipolar coupling and hence the distance between nuclei. Measurement of carbon−fluorine internuclear distances of 12 Å are possible.[26,27]

The dephasing of magnetization in REDOR arises from a local dipolar field gradient and involves no polarization transfer.

The location of the chain ends and the extent of interpenetration of the dendrimers were determined by REDOR NMR experiments, by the measurement of dipolar couplings between ^{13}C labels near the chain ends of poly(benzyl ether) dendrimers and an ^{19}F label placed at the focal point (core). The location and mobility of the chain ends are expected to be affected by the nature of the chain ends, the nature of the monomeric repeat units, the rigidity of the structure, the multiplicity of the branch sites, and the environment surrounding the dendrimer. Therefore, to evaluate a dendritic structure in a homogeneous environment, with compatibility between the chain ends and monomeric repeat units, benzyl-terminated poly(benzyl ether) dendrimers (generations 1−5, molecular weights 416−6814 amu) were examined as pure solids. For the fifth-generation dendrimer, which is large enough to possess the unique properties that are typical for dendrimers after adoption of a globular shape,[6,7] the REDOR NMR data were combined with molecular modeling to generate illustrations and measurements of the overall size, shape, density profile, and packing in the solid state. This is the first report of the use of experimental constraints on molecular modeling for the prediction of dendritic structure.

Experimental Section

Synthesis. The labeled dendrimers were prepared by literature procedure[5] with the ^{13}C label incorporated near the chain ends in the first step of dendrimer growth using ^{13}C-methylene-carbon-labeled benzyl bromide. This label was prepared by reduction of [^{13}C]-benzoic acid (Isotec, Inc., Miamisburg, Ohio) with lithium aluminum hydride, followed by reaction of the resulting ^{13}C-labeled benzyl alcohol with carbon tetrabromide and triphenylphosphine. The ^{19}F label was incorporated in the last step of the synthesis by reaction of 4-fluorophenol with the dendritic benzylic bromide, in the presence of potassium carbonate and 18-crown-6. Purifications were achieved by flash chromatography with elution initially by methylene chloride and finally by 10% diethyl ether in methylene chloride. The composition and purity of the products were confirmed by IR, ^{1}H NMR, ^{13}C NMR, ^{19}F NMR, and gel permeation chromatography.

REDOR Instrumentation and Experiments. Powdered dendrimer (100 mg) was packed into high-performance 7.5 mm outside-diameter zirconia rotors fitted with Kel-F spacers and drive cap. Cross-polarization, magic angle spinning spectra were obtained at 4.7 T and room temperature using a four-channel probe[28] with a single 9 mm diameter solenoidal coil which permits ^{1}H, ^{19}F, ^{13}C, and ^{15}N detection or dephasing at 200, 188, 50, and 20 MHz, respectively. Fluorine incorporation into dendrimers was measured by direct ^{19}F NMR detection and calibrated by comparisons to spectra of materials of known fluorine content.[29] REDOR experiments began after a 2.0 ms matched spin-lock cross-polarization transfer from protons to carbons at 50 kHz, followed by proton decoupling at 100 kHz. The sequence repetition time for most experiments was 4 s. The magic angle stators were obtained from Chemagnetics (Fort Collins, CO). A controlled spinning speed of 5000 Hz was used for all REDOR experiments.

The ^{13}C rotational echoes that form each rotor period following a proton to carbon cross-polarization transfer were prevented from reaching full intensity by insertion of two ^{19}F pulses per rotor cycle, one in the middle of the rotor period and the other at the completion of the rotor period. The ^{19}F pulses were applied using an XY8 phase-cycling scheme to suppress offset effects and compensate for pulse imperfections.[30] A single ^{13}C pulse replaced the ^{19}F pulse in the middle

(18) Lescanec, R. L.; Muthukumar, M. *Macromolecules* **1990**, *23*, 2280.

(19) Mansfield, M. L.; Klushin, L. I. *Macromolecules* **1993**, *26*, 4262.

(20) Naylor, A. M.; Goddard, W. A., III; Kiefer, G. E.; Tomalia, D. A. *J. Am. Chem. Soc.* **1989**, *111*, 2339.

(21) Murat, M.; Grest, G. S. *Macromolecules* **1996**, *29*, 1278.

(22) Hawker, C. J.; Farrington, P. J.; Mackay, M. E.; Wooley, K. L.; Fréchet, J. M. J. *J. Am. Chem. Soc.* **1995**, *117*, 4409.

(23) Percec, V.; Chu, P.; Ungar, G.; Zhou, J. *J. Am. Chem. Soc.* **1995**, *117*, 11441.

(24) Kowalewski, T.; Fields, H. R.; Wooley, K. L. Unpublished results.

(25) Gullion, T.; Schaefer, J. *Adv. Magn. Reson.* **1989**, *13*, 57.

(26) Holl, S. M.; Marshall, G. R.; Beusen, D. D.; Kociolek, K.; Redlinski, A. S.; Leplawy, M. T.; McKay, R. A.; Vega, S.; Schaefer, J. *J. Am. Chem. Soc.* **1992**, *114*, 4830.

(27) McDowell, L. M.; Lee, M.; McKay, R. A.; Anderson, K. S.; Schaefer, J. *Biochemistry* **1996**, *35*, 3328.

(28) Holl, S. M.; McKay, R. A.; Gullion, T.; Schaefer, J. *J. Magn. Reson.* **1990**, *89*, 620.

(29) Pan, Y. *Solid State Nucl Magn. Reson.* **1995**, *5*, 263.

(30) Gullion, T. G.; Baker, D. B.; Conradi, M. S. *J. Magn. Reson.* **1990**, *89*, 479.
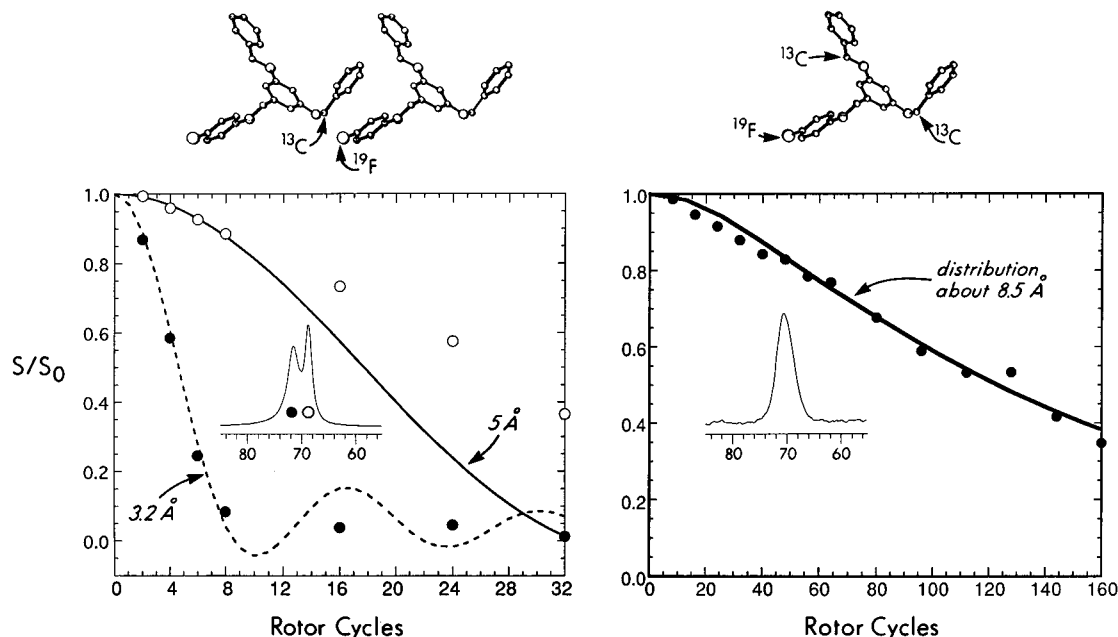
Figure 1. REDOR dephasing by ^{19}F of the methylene-carbon line of undiluted, crystalline, ^{13}C-labeled G1 (left) and a homogeneous mixture of one part of ^{13}C-labeled G1 and nine parts of polystyrene (right). The calculated dephasings for a single ^{13}C$-^{19}$F pair (next-nearest neighbor effects not included) with internuclear separations of either 3.2 or 5.0 Å are shown on the left and those for a Gaussian distribution (5$-$15 Å) centered at 8.5 Å are on the right. The chemical shifts for the two labeled methylene carbons of crystalline G1 are resolved (insert, left). Magic angle spinning was at 5 kHz.

of the evolution period to refocus ^{13}C chemical shifts. When many ^{13}C spins are present, the use of only one ^{13}C pulse minimizes effects of homonuclear coupling.[31] The REDOR difference (the difference between a ^{13}C NMR spectrum, S, obtained under these conditions and one obtained with no ^{19}F pulses, S_0) has a strong dependence on the dipolar coupling and hence the inverse cube of the internuclear distance.

Modeling. For molecular dynamics simulations, Newton's equations of motion were integrated numerically using the Verlet algorithm[32] with a time step of 1 fs and constant NVE. The united-atom model together with the CHARMM potential of Quanta 4.0 (Biosym Molecular Simulation, San Diego, CA) were employed for all calculations. Electrostatic energies were treated with a distance-dependent dielectric constant of 4 and truncated at a cutoff distance of 8 Å. The harmonic potential $k(r - r_o)^2$ was used in the constraint minimizations and molecular dynamics simulations; k is the force constant, r is the instantaneous distance as a function of time, and r_o is the constrained distance. Computations were performed using a Silicon Graphics Power Challenge. A 20 ps simulation for a seven-molecule G5 cluster with 3577 atoms required 5 h of CPU time on an R8000 processor.

Results and Discussion

Rotational-Echo Double-Resonance Applied to Dendrimers. Packing in the crystal for the first-generation structure G1 results in much shorter inter- than intramolecular distances between ^{19}F and the two labeled methylene carbons as determined by X-ray crystallography.[33] The shortest intermolecular distances are 3.2 and 5.0 Å, and the shortest intramolecular distances are 10.0 and 12.1 Å. Thus, essentially full dephasing by ^{19}F is observed in less than about 10 ms for both kinds of chemically distinct carbons in labeled G1 (Figure 1, left). The 72 ppm line is completely dephased after 8 rotor cycles, corresponding to a ^{13}C$-^{19}$F distance of about 3 Å. The dephasing of the 69 ppm line is slower, and the initial rate suggests an average distance of the order of 5 Å. Attempts to

cocrystallize G1 with nonfluorinated versions of the molecule were unsuccessful. However, dilution of G1 in polystyrene (freeze dried from a benzene solution) eliminates the fast dephasing associated with G1 aggregates and therefore proves that the mixing is microscopically homogeneous (Figure 1, right). On the basis of observed distribution of isotropic chemical shifts and ^{13}C$-^{19}$F dipolar couplings (Figure 1, right), G1 adopts a wide range of local conformations in polystyrene.

The broad 70 ppm methylene-carbon line for undiluted, amorphous ^{13}C-labeled G3 (Figure 2) indicates a distribution of local conformations for this higher-generation dendrimer as well. The increased size of G3 means that at least some of the labeled methylene carbons should be farther removed from the fluorine label than the corresponding methylene carbons of labeled G1. Nevertheless, the S/S_o for G3 is 0.75 after 32 rotor cycles (Figure 2, top and middle; Figure 3, bottom), which represents more dephasing than that observed for diluted G1 (Figure 1, right). This result suggests the occurrence of either inward-folding of the chain ends or intermolecular ^{13}C$-^{19}$F dipolar coupling.

Self-dilution of ^{13}C- and ^{19}F-labeled dendrimers by an excess of unlabeled dendrimers is practical for noncrystalline G3, G4, and G5. Dephasing for the diluted labeled dendrimers arises exclusively from intramolecular dipolar coupling, while dephasing for the undiluted samples is due to a combination of intramolecular and intermolecular dipolar couplings. Evaluation of the REDOR data of only the self-diluted samples, shows that the intramolecular dephasings by ^{19}F for ^{13}C-labeled G3, G4, and G5 are comparable and are slightly less than 20% after 32 ms (160 rotor cycles, Figure 3). Some insights into the nature of the distribution are possible from the dependence of S/S_o on the number of rotor cycles. For example, a structure for G4 that has a distribution of the 16 ^{13}C$-^{19}$F distances given by two at 4.4 Å, two less than 10 Å, and the rest over 20 Å, would result in 13% dephasing by ^{19}F in less than 40 rotor cycles, 25% dephasing in 120 rotor cycles, and little further dephasing between 120 and 160 rotor cycles.[34] The observed values are 5% in 40 rotor cycles, 10% in 120 rotor cycles, and no indication

(31) Gullion, T.; Vega, S. *Chem. Phys. Lett.* **1992**, *194*, 423.

(32) Allen, N. P.; Tildesley, D. J. *Computer Simulation of Liquids*; Clarendon Press: Oxford, 1989.

(33) The crystal structure was determined by Alicia Beatty of the X-ray Crystallography Facility, Department of Chemistry, Washington University, St. Louis, MO.
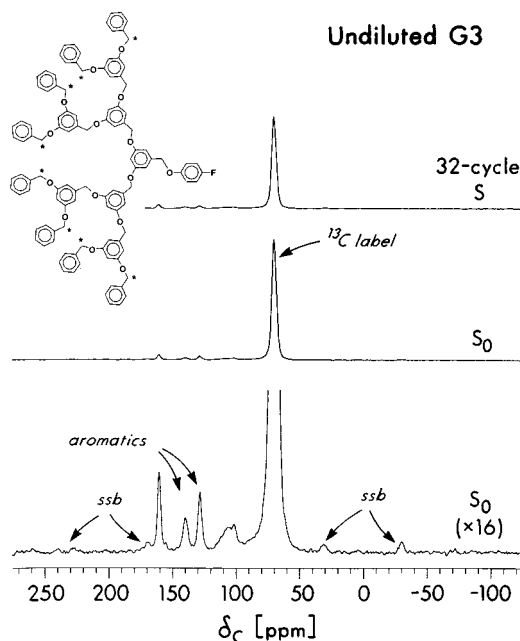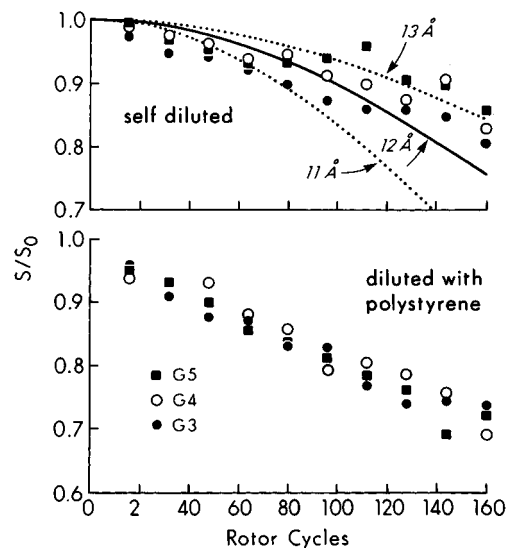
Figure 2. REDOR full-echo (S_o) and dephased (S) ^{13}C NMR spectra of undiluted, amorphous ^{13}C-labeled G3 with magic angle spinning at 5 kHz. The spectra are dominated by the signal at 70 ppm from the eight ^{13}C-labeled methylene carbons per molecule. Aromatic-carbon signals from natural-abundance ^{13}C appear between 110 and 160 ppm. Spinning sidebands are designated "ssb."
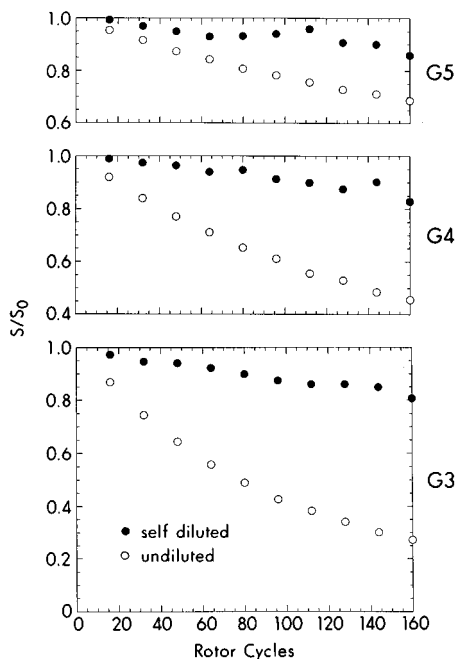
Figure 3. REDOR dephasing by ^{19}F of the methylene-carbon line of undiluted, ^{13}C-labeled G3, G4, and G5 (open circles) and of a homogeneous mixture of one part each of ^{13}C-labeled G3, G4, and G5 and nine parts of the corresponding ^{13}C- and ^{19}F-unlabeled dendrimer (closed circles). Magic angle spinning was at 5 kHz; 160 rotor cycles of dipolar evolution correspond to 32 ms of dephasing.

of a plateau (Figure 3, middle panel). This kind of structure is therefore not a likely candidate to describe G4. Instead, the uniform, monotonic decrease of S/S_o as a function of the number of rotor cycles of dephasing suggests a modest distribution of ^{13}C$-^{19}$F distances with an average of about 12 Å (Figure 4, top). The fact that G3, G4, and G5 all have the same 12 Å

(34) Tong, G.; Pan, Y.; Afeworki, M.; Poliks, M. D.; Schaefer, J. *Macromolecules* **1995**, *28*, 1719.

Figure 4. REDOR dephasing by ^{19}F of the ^{13}C-labeled, methylene-carbon line of a homogeneous mixture of one part each of ^{13}C-labeled G3 (closed circles), G4 (open circles), and G5 (closed squares) and nine parts of either the corresponding ^{13}C- and ^{19}F-unlabeled dendrimer (top) or polystyrene (bottom). Solid and dotted lines show the calculated dephasings for single ^{13}C$-^{19}$F pairs.

average is only consistent with increasing inward-folding of the chain ends with increasing generation number.

The decrease of the intermolecular contributions to dephasing with increasing generation number (comparison of open and closed circles, Figure 3) supports a transition from an open structure with significant intermolecular interpenetration of dendrimer chain ends (contributing to the measurements of more rapid dephasing through shorter intermolecular ^{13}C$-^{19}$F dipolar couplings) for G3 and G4 to a more closed structure with the intradendrimer chain ends filling more of the space around the core for G5.

The more rapid dephasing observed for the polystyrene diluted materials, in comparison to that of the self-diluted samples (Figure 4), suggests a more collapsed structure for the dendrimers in polystyrene. About a 10% decrease in the average ^{13}C$-^{19}$F distance is observed for G3, G4 and G5. This shrinkage is most likely due to incompatibility between the benzyl ether dendrimers and polystyrene. The theoretical model[21] of dendrimers in solution predicts an increase in density with decreasing solvent quality.

The homogeneous T_2 for the full-echo signal of the labeled methylene carbons of G3 is 8.3 ms, increasing to 14.2 ms for G5 (data not shown). Echo-train lifetimes of the order of 10 ms for methylene carbons indicate the absence of large-amplitude motions in the low-kHz regime.[35] Neither slow cross-polarization transfer rates nor unusually fast spin-lattice relaxation rates were observed, indicating the absence of large-amplitude molecular motions even though the room temperature NMR measurements were close to the glass-transition temperatures for G3, G4, and G5 of 32, 39 and 42 °C, respectively.

Molecular Modeling Constrained by REDOR Distances. A computer-generated G5 structure was relaxed by a 20 ps molecular dynamics simulation at 1000 K, followed by 100 and 200 steps of steepest-descent and conjugate-gradient energy minimizations for quenching, respectively. The energy minimizations were performed such that all ^{13}C$-^{19}$F distances that were initially greater than 20 Å were constrained to distances of less than 18 Å using a force constant of 50 kcal/mol. The

(35) Lee, P. L.; Kowalewski, T.; Poliks, M. D.; Schaefer, J. *Macromolecules* **1995**, *28*, 2476.
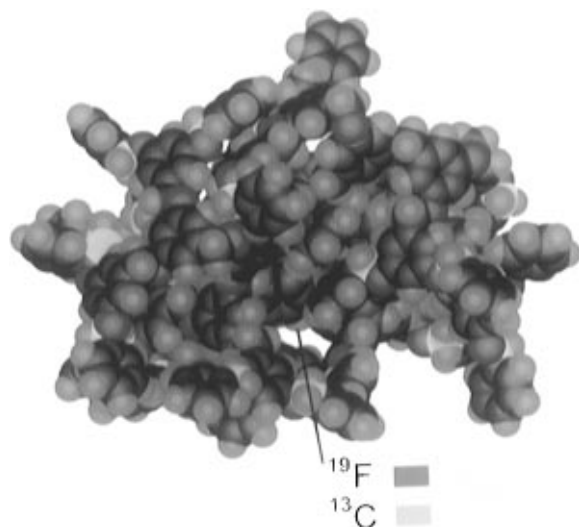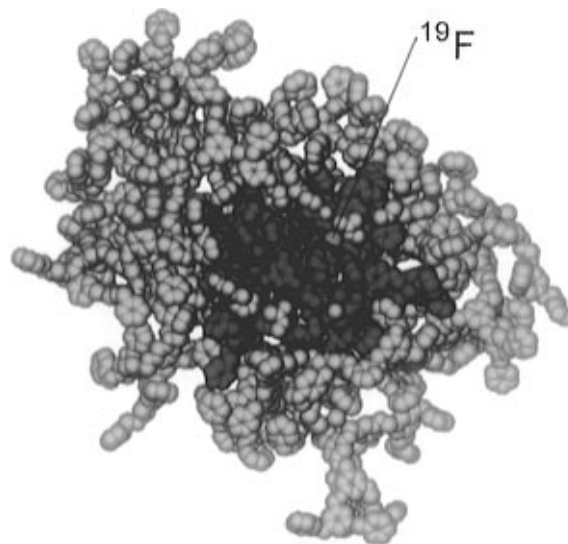
Figure 5. Space-filling rendition of a structure for an isolated G5 dendrimer obtained by a distance-constrained energy minimization. Color code: black, carbon; yellow, ^{13}C-labeled carbon; red, oxygen; blue, hydrogen; cerise, fluorine.

distances to the 32 labeled methylene carbons in the resulting structure (Figure 5) range from 8 to 18 Å, consistent with the observed intramolecular contributions to REDOR dephasing. The fluorine is encapsulated in this simulated quenched structure, which has an ellipsoidal shape and overall dimensions of 31 × 37 × 41 Å.

Intermolecular packing was explored by surrounding the G5 structure of Figure 5 by six neighboring, identical G5 structures in a face-centered cubic (fcc) array to make a seven-molecule cluster. A 500-step energy minimization for the entire cluster preceded a 20-ps molecular dynamics simulation performed in the gas phase at 300 K. Intra- and intermolecular constraints were imposed based on the REDOR distance results of Figures 3 and 4. These ^{13}C–^{19}F distances were imposed both during the energy minimization and the molecular dynamics simulation. The intramolecular constraints were unchanged from the isolated molecule calculation. For the intermolecular constraints, each labeled carbon of the central G5 was required to be within 13 Å of at least one of the surrounding six fluorines using a force constant of 50 kcal/mol. This requirement was designed to produce intermolecular contributions to REDOR dephasing that would be about equal to intramolecular contributions. Because the fluorine of G5 is not in the center of the molecule (see insert, Figure 2), requiring intermolecular ^{13}C dephasing by the neighbor with the most distant fluorine was not practical. For this fluorine, five of the labeled methylene carbons of the central G5 were required to be within 12 Å, which guaranteed significant intermolecular REDOR dephasing by the most remote fluorine even though the majority of ^{13}C labels of the central G5 might be too distant to be affected. The intermolecular constraints ensured that the seven-member G5 cluster would stay together throughout the 20 ps molecular dynamics simulation. Other reasonable starting conditions and REDOR-consistent constraints can be imagined.

The results of the simulation are shown in Figure 6. Twenty-six of the thirty-two ^{13}C labels of the central G5 are between 7 and 17 Å from the fluorine of the central molecule; three are more distant and three are less distant. The shape of the central G5 is the same as that resulting from the isolated-molecule energy minimization, with the ^{19}F label at the core totally encapsulated. All 32 ^{13}C labels of the central G5 are within 17 Å of at least one fluorine on another molecule; most have two or three fluorines within this range, and fifteen of the ^{13}C labels

Figure 6. Space-filling rendition of a structure for a seven-molecule G5 cluster obtained by a 20 ps, distance-constrained, molecular dynamics simulation. The central G5 is shown in red and its neighbors are shown in yellow. A slice through the approximate center of the cluster has been made to reveal the fluorine (in blue green) of the central G5. Most of the atoms of the central G5 are either internal with no contact with a neighboring molecule or are on an interface with only surface contact, but a few are mixed with the atoms of a partially interpenetrating neighboring molecule.
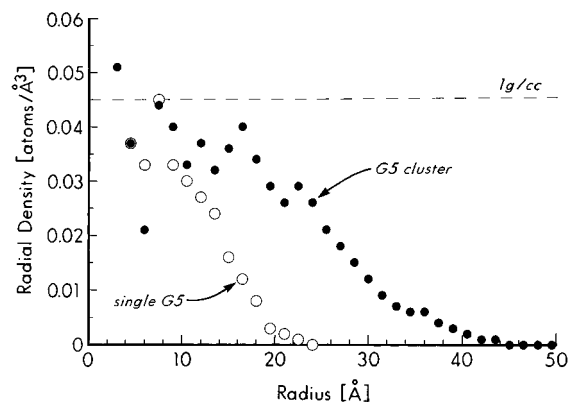
Figure 7. Radial number densities (atoms Å^{-3}) for the isolated G5 dendrimer of Figure 5 (open circles) and for the seven-molecule G5 cluster of Figure 6 (closed circles). The radial number densities were obtained by counting the number of C(H$_n$) and O atoms of the dendrimer repeat unit in the volume between spherical shells separated by 1.5 Å in radius as a function of increasing radius. Spheres were centered at the center of mass of the total structure. Equivalent density distributions for the G5 cluster were obtained from single snapshots at 10, 17.5, and 20.0 ps of the distance-constrained molecular dynamics simulation, as well as from 2.5 ps, 50-point averages between 10 and 20 ps. The dashed line indicates a density of 1 g/cc, assuming an effective atomic mass of 13.4 atomic mass units.

are 13 Å or less from fluorines on other molecules. The central molecule of the G5 cluster therefore is qualitatively consistent with all the intra- and intermolecular constraints derived from the G5 REDOR dephasing results of Figure 3.

Density Profiles for Dendrimers in the Solid State. The radial density profiles for the G5 dendrimer and the seven-molecule dendrimer cluster are plotted in Figure 7. The radial number densities (number of atoms/Å^3) were obtained by counting the number of C(H$_n$) and O atoms of the dendrimer repeat unit in the volume between spherical shells differing in radius by 1.5 Å as a function of increasing radius. The origin of each shell was the center of mass of the total structure. Ignoring statistical scatter for a radius of less than 5 Å, we see

that the radial density for the single G5 dendrimer decreases monotonically with increasing distance from the center of mass, consistent with all of the theoretical predictions cited earlier,[18−21] except that of de Gennes and Hervet.[17] However, a comparison of the radial density of a single G5 molecule and the G5 cluster emphasizes that this decrease in density for a single G5 is largely the result of the sampling for a molecule of finite size. The radial density for the G5 cluster, which is everywhere greater than that of the isolated G5 (Figure 7), is approximately constant and close to 1 g/cc throughout the center of the packed structure (radius between 8 and 18 Å). The density decreases near the periphery because the population of chain ends has been reduced by inward-folding. In solution, this peripheral void space is filled with solvent and, in the solid, by chain ends of other dendrimers.

A density of 1.2 g/cc was measured for an annealed sample of G5. We attribute the approximately 20% difference in density between experiment and simulation mostly to the fact that the simulations were limited to only seven molecules. In addition, the REDOR distances were determined for powdered samples which generally have 5% lower densities than the corresponding annealed glasses. REDOR measurements on annealed dendrimers are in progress. It is also possible that the fcc packing model for the G5 cluster and the limited duration of the simulations underestimated the true packing density.

Conclusions

The proposed molecular model that is based on these REDOR results is representative of a large number of possible conformations, which leads to the definition of an average structure. The size, shape, and packing results generated from the REDOR NMR data combined with molecular modeling for the G5 benzyl ether dendrimer are valid for a flexible and compositionally-compatible structure. Other types of dendrimers, particularly those displaying phase separation or containing rigid monomeric repeat units, could behave differently. We believe that the details of the long-range potentials used in the calculations are not crucial because of the realistic constraints imposed by the long-range experimental distances. The modeling provides estimates of the fraction of atoms in internal, surface, and entangled branches (see Figure 6), and we anticipate that these insights will be important for guiding experiments in drug delivery, DNA binding, and other practical applications of dendrimers. Work in progress in our laboratory includes correlating the microscopic structure of dendrimers obtained from distance-constrained modeling with macroscopic measurements of size, density, and mechanical properties by atomic force microscopy. Future work will involve ^{13}C labeling at specific internal, monomer sites within the dendrimer to obtain additional distances for more closely defined conformational constraints.

JA962285E